

# Extremely low surface recombination in 1 $\Omega$ cm n-type monocrystalline silicon

Ruy S. Bonilla<sup>\*1</sup>, Christian Reichel<sup>2</sup>, Martin Hermle<sup>2</sup>, and Peter R. Wilshaw<sup>1</sup>

<sup>1</sup> Department of Materials, University of Oxford, Parks Rd, OX1 3PH, United Kingdom

<sup>2</sup> Fraunhofer Institute for Solar Energy Systems ISE, Heidenhofstr. 2, 79110 Freiburg, Germany

Received 12 September 2016, revised 24 November 2016, accepted 25 November 2016

Published online 1 December 2016

**Keywords** surface passivation, optoelectronic devices, silicon, solar cells, dielectric materials, coatings

\* Corresponding author: e-mail [sebastian.bonilla@materials.ox.ac.uk](mailto:sebastian.bonilla@materials.ox.ac.uk), Phone: +44 1865 283097, Fax: +44 1865 273777

A key requirement in the recent development of highly efficient silicon solar cells is the outstanding passivation of their surfaces. In this work, plasma enhanced chemical vapour deposition of a triple layer dielectric consisting of amorphous silicon, silicon oxide and silicon nitride, charged extrinsically using corona, has been used to demonstrate extremely low surface recombination. Assuming Richter's parametrisation for bulk lifetime, an effective surface recombination velocity  $S_{\text{eff}} = 0.1 \text{ cm/s}$  at  $\Delta n = 10^{15} \text{ cm}^{-3}$  has been obtained for pla-

nar, float zone, *n*-type, 1  $\Omega$  cm silicon. This equates to a saturation current density  $J_{0s} = 0.3 \text{ fA/cm}^2$ , and a 1-sun implied open-circuit voltage of 738 mV. These surface recombination parameters are among the lowest reported for 1  $\Omega$  cm c-Si. A combination of impedance spectroscopy and corona-lifetime measurements shows that the outstanding chemical passivation is due to the small hole capture cross section for states at the interface between the Si and a-Si layer which are hydrogenated during nitride deposition.

© 2016 WILEY-VCH Verlag GmbH & Co. KGaA, Weinheim

**1 Introduction** Recombination of photo-generated carriers at surfaces and interfaces in optoelectronic devices imposes a major limit to their performance. Minimizing such recombination, also known as passivation, has become a major topic of study as more efficient devices are required. Surface passivation is achieved by using a dielectric coating that often fulfils three tasks: it satisfies dangling bonds at the surface of the underlying silicon thus reducing the number and/or the recombination activity of interface trap states, it provides a fixed electric field that repels a type of carrier preventing its recombination, and it acts as an antireflection coating at the front surface of the cell to enhance light absorption. Recent reports have demonstrated that the passivation quality of a dielectric film can be improved extrinsically, i.e. after-deposition, via a combination of thermal anneals [1, 2], hydrogen exposure [3, 4], and/or dielectric charging [5]. In particular, extrinsically adding charge to a dielectric coating, either from corona charged ions [6] or from charged alkali ions [7], can enhance greatly the passivation properties of the film [8]. A key disadvantage of many extrinsic passivation methods, however, is the lack of their stability [9]. At a practical level, a surface passivation technique must endure the opera-

ting conditions of the device for a length of time as long as that of the device itself. This may require dielectric materials with stable charge over 25 years, also known as electrets [10]. Only in the recent years has the stability issue being tackled with some success [11]. When solved, such electret films may become an essential part in the surface passivation of optoelectronic devices. As evidence of the potential of charged dielectrics, in this work we use corona discharge to produce extremely low surface recombination parameters in monocrystalline silicon (c-Si). A triple layer dielectric film deposited at temperatures below 250 °C has been charged extrinsically using corona discharge to demonstrate outstanding surface passivation of 1  $\Omega$  cm *n*-type c-Si.

**2 Methods** Surface passivation was characterised by producing symmetrical lifetime samples on shiny-etched float zone (FZ) Si wafers,  $\langle 100 \rangle$  surface orientation. The nominal wafer thickness ( $W$ ) was 200  $\mu\text{m}$ . This was measured using a digital linear micrometre resulting in a thickness of  $199 \mu\text{m} \pm 2 \mu\text{m}$ . A thickness of 200  $\mu\text{m}$  was used for the calculations performed here. The nominal wafer resistivity was 1  $\Omega$  cm. This was corroborated using the 4-

probe technique on a  $3 \times 20$  mm<sup>2</sup> sample with four 0.5 mm wide by 3 mm long InGa contacts separated by 5 mm. Resistivity was also measured using the Van der Pauw technique [12] in a rectangular  $5 \times 5$  mm<sup>2</sup> sample. These measurements resulted in a resistivity of  $1.01 \Omega \text{ cm} \pm 2\%$ . A dopant concentration of  $4.9 \times 10^{15} \text{ cm}^{-3}$  was assumed for all the analysis performed here. It is noted here that an accurate estimation of surface recombination parameters depends on precise values for the wafer bulk characteristics, as reported above.

A triple layer dielectric coating consisting of hydrogenated amorphous silicon (a-Si), silicon oxide (SiO<sub>x</sub>), and silicon nitride (SiN<sub>x</sub>) was deposited using plasma enhanced chemical vapour deposition (PECVD). a-Si was deposited in a PlasmaLab 100 system from Oxford Instruments at a temperature of 200 °C, using silane SiH<sub>4</sub> and hydrogen H<sub>2</sub> as precursor gases. SiO<sub>x</sub> and SiN<sub>x</sub> were deposited in an industrial-type in-line PECVD system (Roth & Rau SiNA XS), at a temperature of 250 °C. Silane SiH<sub>4</sub>, nitrous oxide N<sub>2</sub>O and ammonia NH<sub>3</sub> were used as precursor gases, and the gas-flux ratio was optimised to achieve a refractive index of  $n_{\text{SiO}_x} = 1.45$  in the oxide, and  $n_{\text{SiN}_x} = 2.15$  in the nitride at  $\lambda = 632$  nm, as described in reference [13]. The a-Si/SiO<sub>x</sub>/SiN<sub>x</sub> film thicknesses were  $8 \pm 1$  nm/ $13 \pm 2$  nm/ $60 \pm 1$  nm as measured using spectroscopic ellipsometry. After deposition, corona charge was deposited on both sides of the wafer by placing it under a point electrode held at 30 kV, 20 cm above the sample, in laboratory conditions. Further details on this process can be found in [14]. Surface charge concentration was assessed using Kelvin Probe (KP) surface potential measurements [15].

The interface electrical characteristics were measured using frequency dependent capacitance-conductance-voltage (CGV) measurements using a Keysight E4980A precision LCR meter. The top contact was created by thermally evaporating  $\sim 100$  nm of Al through a contact mask, with the area of the contact measured using an optical microscope to within 5% accuracy. The back contact was created using a gallium–indium eutectic. Interface trap density  $D_{\text{it}}$  was determined using the Nicollian and Goetzerberger conductance method [16] without any surface potential fluctuations. The insulator capacitance was determined using the McNutt–Sah method [17] with the extension in [18], and used to calculate the effective oxide thickness as  $\text{EOT} = \epsilon_0 K_{\text{SiO}_2} \text{Area} / C_{\text{ins}}$ . The flatband voltage  $V_{\text{fb}}$  was found by correcting the measured gate voltage  $V_g$  to account for the stretching produced by interface states  $D_{\text{it}}$  and fitting the corrected curve with a theoretical model as proposed in [19].

Surface passivation was quantified using several parameters. Firstly, the effective surface recombination velocity  $S_{\text{eff}} = W/2(1/\tau_{\text{eff}} - 1/\tau_{\text{int}})$ , with  $\tau_{\text{int}}$  defined by Richter's parametrisation (Eq. (18) in [20] using  $B_{\text{rel}}$  from [21] and  $B_{\text{low}}$  from [22]) and  $\tau_{\text{eff}}$  measured experimentally using a Sinton photoconductance decay (PCD) instrument. A WCT 120 instrument was used with an accuracy of 8% as reported in [23]. This accuracy was the main source of error

and was used here to quantify the error bars in the reported data. Secondly, an upper limit to the surface recombination velocity (SRV) was calculated by assuming  $\tau_{\text{Bulk}} \rightarrow \infty$  such that  $S_{\text{UL}} < W/(2\tau_{\text{eff}})$ . This removes the dependence of the inferred value on the empirical relation for bulk lifetime. Thirdly, the surface recombination current  $J_{0s}$  [24], calculated here using approximation (5) in [25], since for high lifetimes Kane and Swanson's method produces non-physical negative recombination currents. Lastly, the implied open-circuit voltage  $i-V_{\text{oc}}$  from the measured photoconductance decay curve was determined as described by Kerr in [26].

**3 Results and discussion** The chemical and field effect components of passivation in the a-Si/SiO<sub>x</sub>/SiN<sub>x</sub> stack were studied by producing specimens without the SiO<sub>x</sub> and/or the SiN<sub>x</sub> layers. In a single layer of a-Si, CGV measurements were not possible due to the conductivity of the film leading to large leakage current errors. Samples with a double layer of 8 nm a-Si/100 nm SiO<sub>x</sub>, and a triple layer of 8 nm a-Si/13 nm SiO<sub>x</sub>/60 nm SiN<sub>x</sub> showed lower leakage and allowed CGV measurements. Figure 1a shows a subset of the CGV spectra for the triple and double layer systems, while Fig. 1b illustrates the resulting  $D_{\text{it}}$  calculated therefrom, in three samples. The solid lines in Fig. 1a show the theoretical model fitted to the conductance to angular frequency functions measured. No Gaussian dispersion was included here to account for fluctuations in the semiconductor surface potential. Despite this, the good fits obtained near the peak indicate good accuracy in the determination of  $D_{\text{it}}$  since it is the magnitude and frequency of the peak the parameters that relate to  $D_{\text{it}}$  [27, 28]. Figure 1b shows that the a-Si/SiO<sub>x</sub> presents a higher concentration of interface states than the a-Si/SiO<sub>x</sub>/SiN<sub>x</sub> film. In both cases the  $D_{\text{it}}$  has been found to exceed  $10^{11} \text{ cm}^{-2} \text{ eV}^{-1}$  suggesting that substantial recombination activity could arise at these interfaces. It is, however, possible that the trap states sampled using the CGV method are at the a-Si/SiO<sub>x</sub> interface, or even in the a-Si bulk.

The flatband voltages obtained for the double a-Si/SiO<sub>x</sub>, and triple a-Si/SiO<sub>x</sub>/SiN<sub>x</sub> layers are  $-0.506$  V, and  $-0.71$  V, respectively. Such low  $V_{\text{fb}}$  indicates a minimal concentration of charge inside the film. The KP surface potential for these two structures was  $-0.31$  V and  $-0.53$  V, respectively, thus indicating very small charge concentrations at the surface of the film. The  $V_{\text{fb}}$  can be used to estimate an intrinsic charge of  $\sim 5 \times 10^{10} \text{ q/cm}^2$  and  $\sim 2.1 \times 10^{11} \text{ q/cm}^2$  respectively, assuming all charge resides at the dielectric/silicon interface. These values are the average of three measurements taken in different specimens. It is noted that contrary to previous reports [29], the oxide/nitride interface in this work did not reveal a large concentration of positive charge.

The minority carrier lifetime in all three coatings has been measured using transient photoconductance, Figure 2a. The surface passivation provided by a single a-Si layer increases the lifetime to over 1 ms. Large leakage cur-

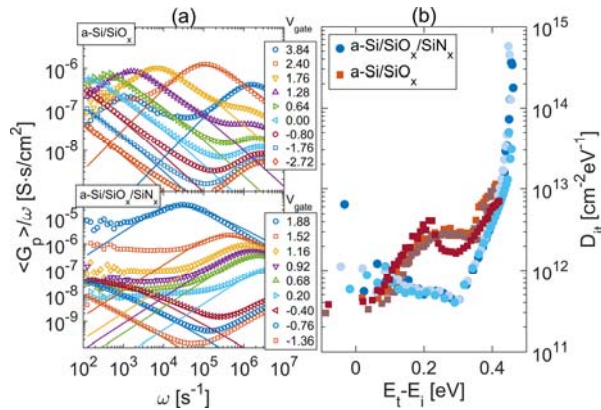


**Figure 1** (a) CGV measurements of the double and triple dielectric systems on Si. (b) Calculated interface state density using the conductance method in three specimens of the double and triple layers.

rents prevented meaningful CGV measurements to assess charge in the a-Si layer. Despite this, the film conductivity would suggest a minor contribution from field effect [30], making the passivation mainly of chemical origin [31, 32]. Since the oxide and nitride layers were deposited at 250 °C in the triple layer system, the a-Si would have been exposed to an additional anneal. To replicate this, the single a-Si layer was annealed at the same temperature for 20 minutes, which increased the effective lifetime to ~4 ms, possibly due to a further hydrogenation of Si bonds. Once the SiO<sub>x</sub> layer is deposited, a reduction in the passivation quality is observed, red trace in Fig. 2a. This can arise from either a high temperature loss in the hydrogen content of the a-Si film, or from plasma damage during the oxide deposition. Since the 250 °C post-deposition anneal applied to the a-Si single layer improved its lifetime, it is likely that the loss in passivation during SiO<sub>x</sub> deposition is due to plasma radiation and/or ion bombardment damage. When the third nitride layer is deposited to form the a-Si/SiO<sub>x</sub>/SiN<sub>x</sub> system, the passivation is largely improved as evidenced from  $\tau_{eff} \sim 3$  ms. In this case, the passivation quality achieved directly after deposition, termed here intrinsic, is mainly of chemical origin with a minor contribution from field effect, as seen from the charge concentration inferred from CGV measurements. This suggests that the a-Si/Si interface is hydrogenated during the PECVD nitride deposition reducing its recombination activity.

The field effect passivation in these films was modified extrinsically using corona discharge. In a single a-Si layer the high conductivity led to a rapid leakage of the corona deposited charge, thus no change in lifetime was observed when attempting to charge this film. On the a-Si/SiO<sub>x</sub> and a-Si/SiO<sub>x</sub>/SiN<sub>x</sub> systems, on the other hand, corona charge modified strongly the field effect passivation as illustrated in Fig. 2b. When the field effect component of passivation was maximised, effective lifetimes as high as 3 ms and 7 ms were recorded in the double and triple layers, respec-

tively. The best passivation achieved is shown by the red and blue solid traces in Fig. 2a.

The solid lines in Fig. 2b illustrate a theoretical model of effective lifetime using an extended Shockley–Read–Hall formalism with the parameterisations in Ref. [33]. The values for the parameters are included in the figure. These show that a concentration of  $\sim 10^{12} cm^{-2}eV^{-1}$  charged donor and acceptor interface states is necessary to explain the observed dependence. This is in agreement with the substantial concentration of interface states measured using CGV, Fig. 1. A combination of CGV and corona-lifetime measurements thus suggests that, when compared to a Si/SiO<sub>2</sub> interface [34], the passivation provided by the a-Si film, and its subsequent hydrogenation, is related to a strong reduction in the capture rate of holes at the interface states, rather than a reduction in the number of states. This is equivalent to a reduction in the capture cross section of holes since the fundamental hole capture rate is given by  $S_{p0} = v_{th}\sigma_p D_{it}$ .

The intrinsic bulk lifetime limit  $\tau_{intb}$ , as calculated from Richter's parametrisation [20], is included in the red solid line in Fig. 2a. In the high injection regime the measured effective lifetimes exceeded this assumed intrinsic limit. The work of Wan et al. [35] is the only other report where lifetimes exceeding the intrinsic limit are observed, yet in their work 0.47  $\Omega cm$  Si was studied instead. Both in Wan et al. and in this study, experimental effective lifetime is seen to exceed the assumed radiative and Auger limit. Error bars for the effective lifetime measured here were calculated considering the accuracy reported in [23] and included in Fig. 2a. The intrinsic limit deduced from Richter's parameterisation falls within these error bars. However, for the  $\Delta n > 10^{15} cm^{-3}$  regime, the lifetimes measured fall in the top 50% percentile, suggesting that lifetimes surpassing the assumed intrinsic limit are likely.

The surface recombination parameters of these specimens were calculated as described in Section 2. Figure 3 illustrates the calculated SRV and currents, including the errors from both lifetimes and thickness measurements. Here

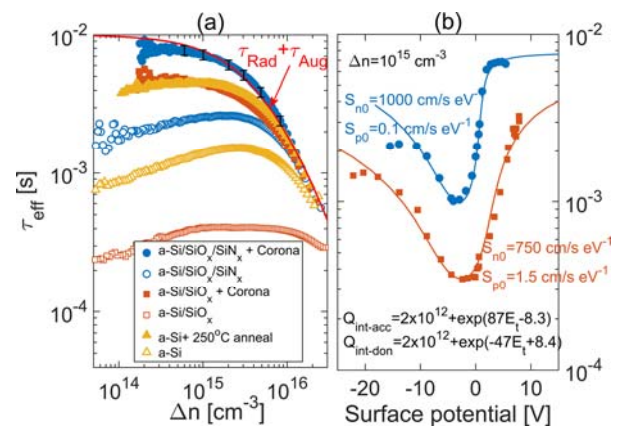


**Figure 2** Transient photoconductance decay lifetimes as a function of (a) injection level and (b) surface potential, for n-type Si extrinsically passivated with corona charge.



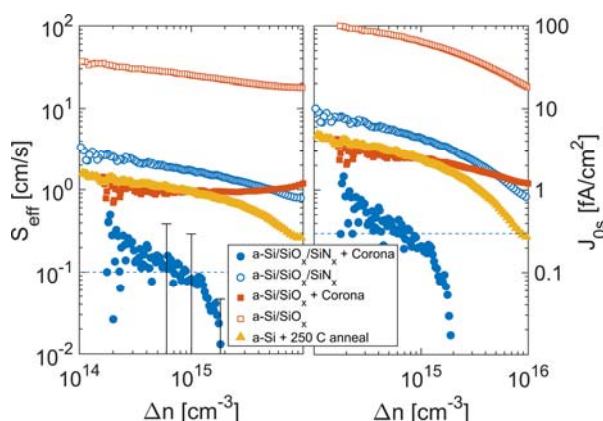


**Figure 3** Effective surface recombination velocity (left) and current density (right) as a function of minority carrier density for the lifetime specimens in Fig. 2.

it is evident that a-Si provides an outstanding base chemical interface to the underlying Si. The SiO<sub>x</sub> provided negligible field effect passivation and affected the chemical passivation achieved from the a-Si alone, yet it was necessary to avoid the leakage of extrinsic corona charge later deposited on the three-layer film. Deposition of the final SiN<sub>x</sub> layer provided additional chemical passivation from hydrogenation taking place during deposition, with a minor contribution from field effect. Once the chemical and the field effect components of passivation are exploited jointly,  $S_{\text{eff}}$  and  $J_{0s}$  of 0.1 cm/s and 0.3 fA/cm<sup>2</sup> are observed at an injection level of 10<sup>15</sup> cm<sup>-3</sup>. The calculated 1 sun i- $V_{\text{oc}}$  for such specimen was 738 mV. It is noted that for such low recombination, these parameters are strongly dependent on the Auger and radiative lifetime models used. It is clear that if the parametrisation of Auger recombination is modified these surface recombination parameters will change substantially. In other reports this has been avoided by assuming zero bulk recombination and quoting an SRV upper limit. Such calculation has been here included in Table 1 for  $\Delta n = 10^{15}$  cm<sup>-3</sup>. Here the recombination parameters, calculated as stated in Section 2, are listed for state-of-the-art passivation methods reported in the literature. The values achieved in this work have been included for comparison. It is clear that the results in this work are among lowest recombination observed for a 1  $\Omega$  cm (100) Si surface. Similarly low surface recombination was reported by Herasimenka in 2013 [36] yet their work was done on higher resistivity silicon. Additionally, the oxide and nitride layers here reported were deposited using an inline industrial system.

**4 Conclusions** This letter reports one of the lowest surface recombination parameters recorded using PCD lifetimes. In a float zone n-type 1  $\Omega$  cm silicon specimen, a triple layer dielectric of low temperature PECVD a-Si/SiO<sub>x</sub>/SiN<sub>x</sub> provides outstanding chemical passivation, mainly due to the reduced hole capture rate provided by the a-Si layer and its hydrogenation during nitride deposi-

**Table 1** State of the art surface passivation methods on ~1  $\Omega$  cm n-type FZ Si. Values reported at  $\Delta n = 10^{15}$  cm<sup>-3</sup>.

method	$\rho$ [ $\Omega$ cm]	$\tau_{\text{eff}}$ [ms]	$S_{\text{eff}}$ [cm/s]	$S_{\text{UL}}$ [cm/s]	$J_{0s}$ [fA/cm <sup>2</sup> ]
annealed SiO <sub>2</sub> [37]	1.5	6	1.36	2.37	4.95
charged SiO <sub>2</sub> [6]	1	5.2	0.65	1.92	1.5
PA-ALD AlO <sub>x</sub> [20]	1	6.8	0.14	1.33	0.37
r-PECVD SiN [20]	1	6.3	0.27	1.58	0.71
a-Si/SiO <sub>x</sub> /SiN <sub>x</sub> [36]	1.7	15	0.114	1	0.29
SiO <sub>2</sub> /PECVD SiN <sub>x</sub> [8]	1	6.7	0.14	1.49	0.36
this work:	1	7.2	0.1	1.38	0.21
a-Si/SiO <sub>x</sub> /SiN <sub>x</sub>					

tion. Further improvement in passivation is demonstrated using corona charge field effect which leads to an effective SRV of 0.1 cm/s, a saturation current density of 0.3 fA/cm<sup>2</sup>, and a 1 sun implied open circuit voltage of 738 mV. Lastly, effective lifetimes exceeding the Auger intrinsic limit parametrised by Richter were observed for the  $\Delta n > 2 \times 10^{15}$  cm<sup>-3</sup> regime.

**Acknowledgements** RS Bonilla is the recipient of an EPSRC (UK) Postdoctoral Research Fellowship, EP/M022196/1. PR Wilshaw acknowledges the support from EPSRC grant EP/M024911/1. Data published in this article can be downloaded from <http://ora.ox.ac.uk>.

## References

- [1] S. Narasimha and A. Rohatgi, Appl. Phys. Lett. **72**, 1872 (1998).
- [2] B. Hoex, S. B. S. Heil, E. Langereis, M. C. M. van de Sanden, and W. M. M. Kessels, Appl. Phys. Lett. **89**, 042112 (2006).
- [3] M. J. Kerr, J. Schmidt, A. Cuevas, and J. H. Bultman, J. Appl. Phys. **89**, 3821–3826 (2001).
- [4] A. Rohatgi, P. Doshi, J. Moschner, T. Lauinger, A. G. Aberle, and D. S. Ruby, IEEE Trans. Electron Devices **47**, 987–993 (2000).
- [5] S. W. Glunz, D. Biro, S. Rein, and W. Warta, J. Appl. Phys. **86**, 683–691 (1999).
- [6] R. S. Bonilla, P. G. Hamer, and P. R. Wilshaw, in: EUPVSEC, Munich, Germany, 2016, pp. 707–710.
- [7] R. S. Bonilla and P. R. Wilshaw, Appl. Phys. Lett. **104**, 232903 (2014).
- [8] R. S. Bonilla, F. Woodcock, and P. R. Wilshaw, J. Appl. Phys. **116**, 54102 (2014).
- [9] J. Schmidt and A. G. Aberle, Prog. Photovolt.: Res. Appl. **263**, 259–263 (1998).
- [10] G. M. Sessler, Electrets, 2nd ed. (Springer, Berlin, 1987).
- [11] R. S. Bonilla, K. Collett, L. Rands, G. Martins, R. Lobo, and P. R. Wilshaw, Solid State Phenom. **242**, 67–72 (2015).
- [12] L. J. van der Pauw, Philips Tech. Rev. **20**, 220–224 (1958).
- [13] J. Seiffé, L. Gautero, M. Hofmann, J. Rentsch, R. Preu, S. Weber, and R. A. Eichel, J. Appl. Phys. **109**, 34105 (2011).
- [14] R. S. Bonilla, C. Reichel, M. Hermle, S. Senkader, and P. Wilshaw, in: IEEE 40th Photovolt. Spec. Conf., IEEE 2014, pp. 0571–0576.

- [15] R. S. Bonilla, N. Jennison, D. Clayton-Warwick, K. A. Collett, L. Rands, and P. R. Wilshaw, *Energy Procedia*, in press (2016).
- [16] E. H. Nicollian and A. Goetzberger, *Appl. Phys. Lett.* **7**, 216 (1965).
- [17] M. J. McNutt and C. T. Sah, *J. Appl. Phys.* **46**, 3909 (1975).
- [18] S. V. Walstra and C.-T. Sah, *Solid State. Electron.* **42**, 671–673 (1998).
- [19] S. M. Sze and K. K. Ng, *Physics of Semiconductor Devices* (Wiley, Hoboken, New Jersey, 2007).
- [20] A. Richter, S. W. Glunz, F. Werner, J. Schmidt, and A. Cuevas, *Phys. Rev. B* **86**, 165202 (2012).
- [21] P. P. Altermatt, F. Geelhaar, T. Trupke, X. Dai, A. Neisser, and E. Daub, in: NUSOD '05, Proc. 5th Int. Conf. Numer. Simul. Optoelectron. Devices, IEEE 2005, pp. 47–48.
- [22] T. Trupke, M. A. Green, P. Würfel, P. P. Altermatt, A. Wang, J. Zhao, and R. Corkish, *J. Appl. Phys.* **94**, 4930 (2003).
- [23] A. L. Blum, J. S. Swirhun, R. A. Sinton, F. Yan, S. Herasimenka, T. Roth, K. Lauer, J. Haunschild, B. Lim, K. Bothe, Z. Hameiri, B. Seipel, R. Xiong, M. Dhamrin, and J.D. Murphy, *IEEE J. Photovoltaics* **4**, 525–531 (2014).
- [24] K. R. McIntosh and L. E. Black, *J. Appl. Phys.* **116**, 14503 (2014).
- [25] H. Mäkel and K. Varner, *Prog. Photovolt.: Res. Appl.* **21**(5), 850 (2013).
- [26] M. J. Kerr, A. Cuevas, and R. A. Sinton, *J. Appl. Phys.* **91**, (2002) 399 (2002).
- [27] E. H. Nicollian and J. R. Brews, *MOS (Metal Oxide Semiconductor) – Physics and Technology* (Wiley, New York, 1982).
- [28] D. K. Schroder, *Semiconductor Material and Device Characterization* (John Wiley & Sons, Inc., 2006).
- [29] R. S. Bonilla, C. Reichel, M. Hermle, and P. R. Wilshaw, *J. Appl. Phys.* **115**, 144105 (2014).
- [30] S. De Wolf, G. Agostinelli, G. Beaucarne, and P. Vitanov, *J. Appl. Phys.* **97**, 63303 (2005).
- [31] S. De Wolf, C. Ballif, and M. Kondo, *Phys. Rev. B* **85**, 113302 (2012).
- [32] S. De Wolf and M. Kondo, *Appl. Phys. Lett.* **90**, 42111 (2007).
- [33] R. S. Bonilla and P. R. Wilshaw, *J. Appl. Phys.*, under review (2016).
- [34] S. W. Glunz, D. Biro, S. Rein, and W. Warta, *J. Appl. Phys.* **86**, 683 (1999).
- [35] Y. Wan, K. R. McIntosh, A. F. Thomson, and A. Cuevas, *IEEE J. Photovolt.* **3**, 554–559 (2013).
- [36] S. Y. Herasimenka, C. J. Tracy, V. Sharma, N. Vulic, W. J. Dauksher, and S. G. Bowden, *Appl. Phys. Lett.* **103**, 183903 (2013).
- [37] M. J. Kerr and A. Cuevas, *Semicond. Sci. Technol.* **17**, 35–38 (2002).